Conduction Electrons in Magnetic Metals

M. S. S. Brooks

European Commission, Joint Research Centre, Institute for Transuranium Elements,
Postfach 2340, D-76125 Karlsruhe, Germany

Abstract

The conduction electrons in magnetic metals are sometimes themselves responsible for the magnetism, as in the $3d$ transition metals, and sometimes are magnetic intermediaries, as in the rare earths. In both cases the calculated magnitude of the exchange interactions is now in good agreement with experiment. The effect of magnetism upon the crystal structure of the $3d$ transition metals is reviewed. In the rare earths the manner in which the conduction electrons mediate the interactions between the $4f$ states is examined by using constrained calculations. The actinides present a more complex problem since there are large orbital contributions to the magnetic moments which are not, as in the rare earths, determined by Russel–Saunders coupling and the Wigner–Eckart theorem.

1 Introduction

Most atoms loose their magnetic moments in the metallic state; the exceptions are some transition metals, the rare earths, and the actinides. The $3d$, $4d$ and $5d$ transition metals, when not magnetically ordered, have relatively large paramagnetic susceptibilities. The magnetism is primarily due to the d-states close to the Fermi energy which are also involved in the determination of cohesion and structure (Friedel, 1969; Pettifor, 1970, 1972). Nearly all of the rare earths are magnetic, the magnetism arising from the orbitally degenerate localized open $4f$-shell (Duthie and Pettifor, 1977; Skriver, 1983a). The rare earth metals are early $5d$-transition metals since the $5d$ shell is less than half-filled and the $4f$ shell chemically inert the bonding and structure being due to the conduction electrons (Jensen and Mackintosh, 1991). The actinides are more complex. The light actinides are $5f$-transition metals while the heavy actinides have an essentially chemically inert $5f$-shell and are therefore early $6d$-transition metals (Skriver, 1985; Wills and Eriksson, 1992; Söderlind et al., 1995).

The $4f$ shell in metallic rare earths is similar to the $4f$ shell of the isolated atom, modified only weakly by interaction with the environment in the solid (Duthie and Pettifor, 1977; Skriver, 1983a). But the exchange interactions between the $4f$ and conduction, principally $5d$, electrons are responsible for the induced conduction electron spin density through which the $4f$-shells interact. Free rare earth and $3d$ transition metal ions are normally described by Russell–Saunders coupling scheme in which Coulomb correlation is the largest part of the ionic valence electron Hamiltonian. Spin–orbit interaction is projected onto eigenstates characterized by total spin and total orbital angular momentum which it couples to give a total angular momentum of $\mathbf{J} = \mathbf{L} + \mathbf{S}$. The saturated ground state $4f$ moment, μ_s^{4f}, is then the product of J with the Landé factor, g_J and the orbital degeneracy of the ground state is partially or fully removed by the crystalline electric field in the solid. One of the most interesting characteristics of rare earths is the interaction between the induced itinerant electron magnetism of the conduction electrons and the localized and anisotropic $4f$ magnetism of the rare earth ions in the elemental metals. Similarly, in rare earth transition metal intermetallics, the nature of the interaction between the transition metal $3d$ magnetism and the localized $4f$ magnetism of the rare earth ions is of primary interest. This has naturally led to investigations of the site-resolved moments which have been studied in neutron diffraction experiments (Boucherle et al., 1982; Givord et al., 1980, 1985) and by theory (Yamada and Shimizu, 1986; Brooks et al., 1989, 1991b) and the coupling between the transition metal and rare earth magnetic moments (Brooks et al., 1991c; Liebs et al., 1993) which transfers magnetic anisotropy to the transition metal.

The magnetic moments of the $3d$ transition metals, in contrast, are due to splitting of the up and down spin states at the Fermi energy which must be calculated self-consistently since both magnetic and kinetic energies are involved (Christensen et al., 1988). In contrast to the rare earth magnetism the orbital magnetism in the $3d$ transition metals is very weak since itinerant states responsible for the magnetism are orbitally non-degenerate, almost totally quenching the orbital moments (Singh et al., 1976; Ebert et al., 1988; Eriksson et al., 1990b).

The light actinide metals are Pauli paramagnets (Skriver et al., 1978, 1980). The heavy actinides (Cm and beyond) are probably localized magnets, similar to the rare earth metals although sound experimental data is sparse. Many actinide compounds, however, order magnetically and there are critical An–An spacings in actinide compounds above which ground state ordered moments are stable (Hill, 1970). The systematic absence of magnetism in compounds with small An–An separation suggests that magnetic ordering is due to the competition between kinetic and magnetic energies and actinide transition metal intermetallics provide several examples of the magnetic transition as a function of either the actinide or the transition metal. But the magnetic actinide compounds have – in contrast to normal transition metals – very large orbital moments (Brooks and Kelly, 1983; Brooks, 1985; Eriksson et al., 1990a,c) since the $5f$ spin-orbit interaction in the actinides is far larger than that of the $3d$ spin–orbit interaction in the much lighter $3d$

transition metals. Figure 1 shows the relative size of the spin–orbit interaction and bandwidths for the transition metals, rare earths and actinides. The bandwidths of the actinides are less than those of the $3d$ transition metals, whereas the spin–orbit interaction is far larger and it mixes an orbital moment into the ground state. This involves mixing states from across the energy bands, and when the bandwidth is large the mixing is small and vice versa. The narrow $5f$ bands and the large spin–orbit interaction in actinides produces the ideal situation for itinerant electrons to support the strong orbital magnetism which is one of the remarkable features of actinide magnetism.

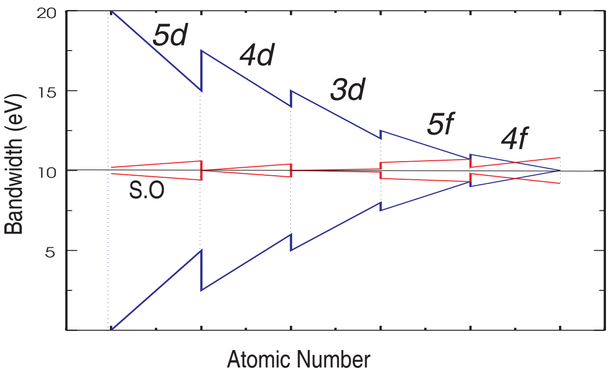

Figure 1. Widths of the d and f bands compared with spin-orbit splitting for the transition metals, rare earths and actinides.

2 Exchange interactions

Density functional theory (Hohenberg and Kohn, 1964; Kohn and Sham, 1965; von Barth and Hedin, 1972) transforms the many-electron problem into an effective one particle problem. Most electronic structure calculations for real materials use a very simple approximation to density functional theory, the local spin density approximation (LSDA), where the exchange and correlation energy is approximated by the sum of local contributions which are identical to those of a homogeneous electron gas at that local density. In LSDA the spin up and spin down states have different potentials which self-consistently arise from the different spin up and spin down densities if the system is magnetic, just as in unrestricted Hartree Fock theory. An approximation to the self-consistent theory is to restrict the spin up and down potentials to the same shape, from which Stoner theory follows with the band splitting at the Fermi energy the product of the magnetic moment and an exchange integral. The exchange integral is simplest if just one angular momentum component contributes, which is a reasonable approximation for transition metals where *d*-states dominate (Gunnarsson, 1976, 1977). The calculated *d*–*d* exchange integrals for transition metals are shown in Fig. 2 (Christensen et al., 1988). The exchange integrals have a minimum inside the series because they are proportional to the integral of the the two thirds power of the reciprocal of the density which leads to a decrease and to the fourth power of the *d*-wave function which increases due to wave function contraction across the series.

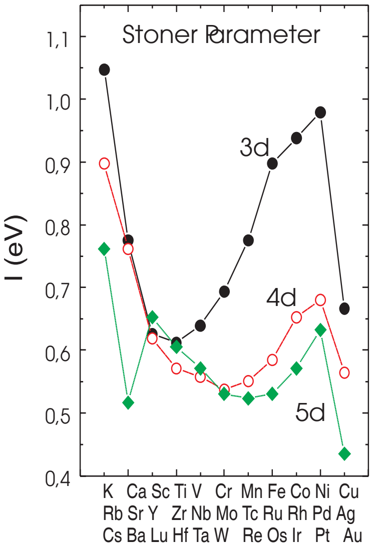

Figure 2. Exchange integrals for the transition metals.

In the Hartree–Fock approximation that part of the exchange energy which depends upon the total spin may be approximated by (Severin et al., 1993)

$$E_{\mathrm{SP}}^{\mathrm{HF}} = -\frac{1}{4}\sum_{ll'} V_{ll'}\mu_l\mu_{l'} \tag{1}$$

in terms of the partial spin moments, μ_l. The exchange integrals $V_{ll'}$ are linear combinations of products of radial Slater exchange integrals and Clebsch–Gordan coefficients. The isotropic exchange interactions $V_{ll'}$ therefore depend only upon the orbital quantum number of the shell and radial integrals. The calculated HF f–d and f–p exchange integrals of free rare earth and actinide atoms are shown in Fig. 3. In LSDA the spin polarization energy may also be expressed in terms of radial exchange integrals (Severin et al., 1993)

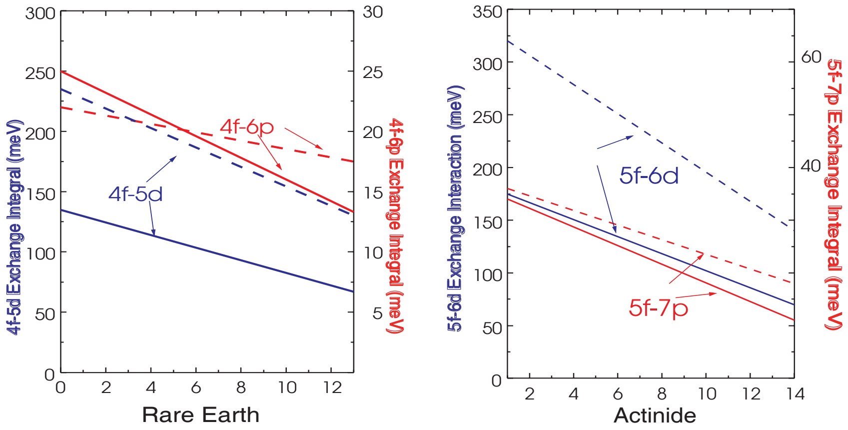

Figure 3. Exchange integrals for free rare earth and actinide atoms from HFA and LSDA.

$$E_{\mathrm{SP}}^{\mathrm{LSDA}} = -\frac{1}{4} \sum_{ll'} J_{ll'} \mu_l \mu_{l'} \,. \tag{2}$$

The f–p and f–d LSDA exchange integrals for the f states of rare earth and actinide atoms are also shown in Fig. 3. The reason that the f–d exchange integrals decrease across each series is the contraction (Lanthanide and Actinide) of the f-shell, which decreases the overlap with the d-states. The overlap between $4f$ and $5d$ densities occurs over a relatively small region of space corresponding to the outer part of $4f$ density and the inner part of the $5d$ density (Fig. 4). As the $4f$ shell contracts the region of overlap decreases. HFA and LSDA yield quite different magnitudes for the f–d exchange integrals which determine the induced conduction electron polarization. Experience has shown that the LSDA integrals lead to splittings of energy bands and calculated magnetic moments that are in better agreement with measurements than if the HF approximation is used.

In the standard model (Duthie and Pettifor, 1977; Skriver, 1983a) for rare earths

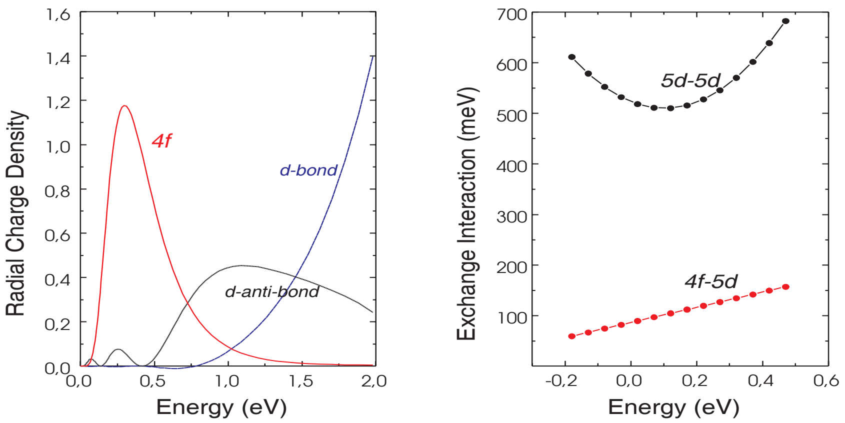

Figure 4. Overlap of the $4f$ and $5d$ charge densities in Gd metal for bonding and anti-bonding $5d$-states.

the exchange interaction Hamiltonian between conduction electrons and local $4f$ moments is

$$H_{s\text{-}f} = -2\tilde{J}_{4f\text{-}c}\mathbf{S}_{4f} \cdot \mathbf{s_c} = -\tilde{J}_{4f\text{-}c}(g_J - 1)\mathbf{J}_{4f} \cdot \boldsymbol{\mu}_c \tag{3}$$

where $\tilde{J}_{4f\text{-}c}$ is an average taken over the ground state J multiplet, $\mathbf{J}_{4f}$ is the total $4f$ angular momentum and $\mathbf{s}_c$ is the conduction electron spin and $\boldsymbol{\mu}_c$ its moment. In rare earth metals and compounds the $5d$ and $6p$ states make larger contributions to the exchange interactions than do the $6s$ states. The exchange integrals are always positive. The spin up and spin down conduction bands are split by the exchange interactions

$$\epsilon^{\pm}_{nk} = \epsilon_{nk} \mp \langle J^z_{4f}\rangle(g_J - 1)\tilde{J}_{4f\text{-}c}(n\mathbf{k}, n\mathbf{k}) \tag{4}$$

leading to an approximate conduction electron moment

$$\langle \mu^z_c\rangle = \mu_B N(\epsilon_F)(g_J - 1)\langle J^z_{4f}\rangle \tilde{J}_{4f\text{-}c} \tag{5}$$

where $N(\epsilon)$ is the state density per f.u. in the paramagnetic phase.

In density functional theory the exchange integrals between $4f$ states and conduction electrons of partial l character are

$$J_{4f\text{-}l}(n\mathbf{k}, n\mathbf{k}) = \frac{2}{3}\int r^2 \phi^2_{4f}(r)\phi^2_l(r, E_{n\mathbf{k}})A[n(r)]/n(r)dr\ , \tag{6}$$

where $A(r)$ is a well known (Hohenberg and Kohn, 1964; Kohn and Sham, 1965; von Barth and Hedin, 1972) function of the density. In the solid state where the conduction electron bands are continuous functions of energy and the exchange integrals are energy dependent. The magnitude of $J_{4f\text{-}5d}$ depends upon the small overlap region of the $4f$ and $5d$ densities (Fig. 4) which varies enormously as the bonding $5d$ density is moved outwards away from the $4f$ density.

The total energy of a system which is allowed to polarize may be separated into a part depending upon the electron density, $E[n]$, and a part depending upon both the density and spin density, $\Delta E[n, \mu]$. Changes in spin density induce changes in the total electron density and in the components of $E[n]$ such as the kinetic energy but $E[n]$ is at a variational minimum in the paramagnetic state therefore the individual components cancel to $o(\delta n^2)$ and make a negligible contribution to the magnetic energy. The remaining energy, $\Delta E[n, \mu]$, may be split into two contributions one of which is the exchange interaction energy and the other is the change in the kinetic energy arising from polarization of the conduction bands. The latter contribution is just $\mu_c^2/2\chi_0$ and is always positive. In transition metals the balance between these two contributions to the magnetic energy is responsible for the Stoner criterion. In the rare earths χ_0 is small and the conduction bands are polarized by the $4f$ states as they would not by themselves polarize. The conduction electron band splitting in the field of the $4f$ states is then given in LSDA by replacing $\tilde{J}_{4f\text{-}c}$ in the standard model by $J_{4f\text{-}c}$. The effective energy splitting at the Fermi energy is (Brooks and Johansson, 1993)

$$\Delta\epsilon(E_F) = \sum_l \left[\frac{N_l(E_F)}{N(E_F)} \sum_{l'} J_{ll'}(E_F)\mu_{l'} + J_{4f\text{-}l}(E_F)\mu_{4f}^s \right], \tag{7}$$

where the sum over l, l' excludes $l = 3$ and q labels the atom. The integrals, $J_{ll'}(E_F)$, for the hcp Gd are calculated to be $J_{5d5d} = 39$ mRy, $J_{5d6p} = 40$ mRy and $J_{5d6s} = 42$ mRy and are more or less constant across the series. The integrals $J_{4f\text{-}d}(E_F)$ varies from 8.6 mRy for Pr to 6.5 mRy for Gd. Since rare earth contraction, which changes $4f$–$5d$ overlap, is fairly smooth the integrals may reasonably be interpolated by $J_{4f\text{-}5d} \approx 8.6 - 0.42(x - 2)$ mRy where x is the number of $4f$ electrons.

Self-consistent calculations for Gd using the linear muffin tin orbital (LMTO) method (Andersen, 1975; Skriver, 1983b) in which the $4f$ spin is varied between 0 and 7 confirm that the $5d$ moment is approximately a linear function of the $4f$ spin. The $5d$ conduction electron moments may be estimated from the corresponding exchange splitting of the $5d$ bands at the Fermi energy, at various levels of approximation. If it is assumed that the partial $5d$ state state density dominates the $5d$ moment at a site is given by

$$\mu_{5d} = J_{4f5d}\mu^s_{4f}\frac{N_{5d}(E_F)/2}{[1 - J_{5d5d}N_{5d}(E_F)/2]}, \tag{8}$$

where J_{5d5d} is calculated to be 531 meV for Gd and $\mu^s_{4f} = 7$ is the $4f$ spin. This approximation yields results to within a few percent of the actual $5d$ moments obtained in the self-consistent spin polarized LMTO calculations (Fig. 5). The partial $5d$ state density at the Fermi energy is calculated to be about 16 states/Ry/atom in the paramagnetic state and is more or less constant across the heavy rare earth series. The $5d$ moment for Gd is calculated to be $\mu_{5d} = 0.53\ \mu_B$ from Eq. (8) and to be $\mu_{5d} = 0.48\ \mu_B$ self-consistently. Self-consistent spin polarized LMTO calculations yield a total conduction electron moment for Gd of 0.65 μ_B which compares well with the measured value of 0.63 μ_B (Roeland et al., 1975) and suggests that LSDA gives reasonable values for the conduction band

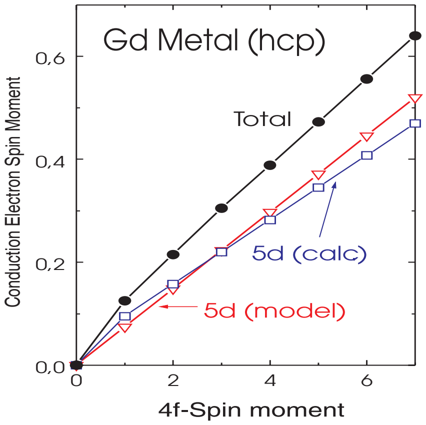

Figure 5. The calculated conduction electron moment in Gd metal as a function of $4f$ spin moment. Also shown are the $5d$ contribution and the $5d$ contribution calculated using the model with exchange interactions.

Wulff et al. (1988) deduced an effective exchange interaction of about 9 mRy from dHvA data for Pr. The calculated exchange interactions are $J_{4f\text{-}5d} = 8.6$ mRy and $J_{5d5d} = 38$ mRy. The partial $5d$ state density is 50 states/cell/Ry compared with a total of 66 states/cell/Ry. The effective $4f$–$5d$ interaction is

$$\bar{J}_{4f\text{-}5d}(E_F) = J_{4f\text{-}5d}(E_F)\frac{N_{5d}(E_F)}{N(E_F)} \tag{9}$$

which is only 6.6 mRy. This interaction is then enhanced by the effective $5d$–$5d$ interaction which, from Eq. (8), is 29 mRy. The enhanced $5d$–$5d$ exchange interaction then becomes 8 mRy, if the $6s$ and $6p$ contributions are neglected.

3 Transition metal magnetism and crystal structure

The crystal structures of the transition metals follow the same structural sequence hcp → bcc → hcp → fcc through the series as a function of atomic number. The origin of the crystal structure sequence is the influence of crystal structure upon the total energy. Although it is difficult to analyse the total energy the force theorem (Pettifor, 1976; Mackintosh and Andersen, 1979) enables total energy differences to be analysed in terms of single electron contributions to the total energy. In particular, structural energy differences are related directly to differences in band contributions to the total energy and therefore to the differences in state densities for the different structures (Pettifor, 1986). The partial d-state densities of the transition metals have a characteristic shape, which follows from canonical band theory and depends only upon structure, independent of series or atomic number (Andersen, 1975; Skriver, 1983b). The shape of a state density, or eigenspectrum, may be characterized – as for any distribution function – by its energy moments (Cyrot-Lackmann, 1967)

$$\mu_m = \mathrm{Tr}\, H^m = \sum_{l_1,l_2,\ldots l_n} H_{l_1 l_2} H_{l_2 l_3} \ldots H_{l_n l_1}\,. \tag{10}$$

The mth moment is therefore obtained from all paths of length m which begin and end at a particular atom. Moments up to the second influence the grosser cohesive properties such as cohesive energy and lattice constant. The second moment, for example, is directly related to the width of a rectangular (or constant) density of states which enters Friedel's model of metallic cohesion. The structure in the density of states which is characteristic of a particular lattice enters through the higher moments which differ significantly between bcc, fcc and hcp structures. If two state densities have identical moments up to the nth moment then the energy difference as a function of band filling must have $(n-1)$ nodes within the bands (Ducastelle and Cyrot-Lackmann, 1971). The bcc state density splits into distinct bonding and anti-bonding regions with a minimum for 6 states (Fig. 6). The fcc and hcp state densities have less pronounced bonding and anti-bonding regions and are broadly similar but differ in that the hcp state density has local minima for 4 and 8 states. The bimodal character of the bcc state density is due to its relatively small fourth moment and it implies that the band energy contribution of the bcc

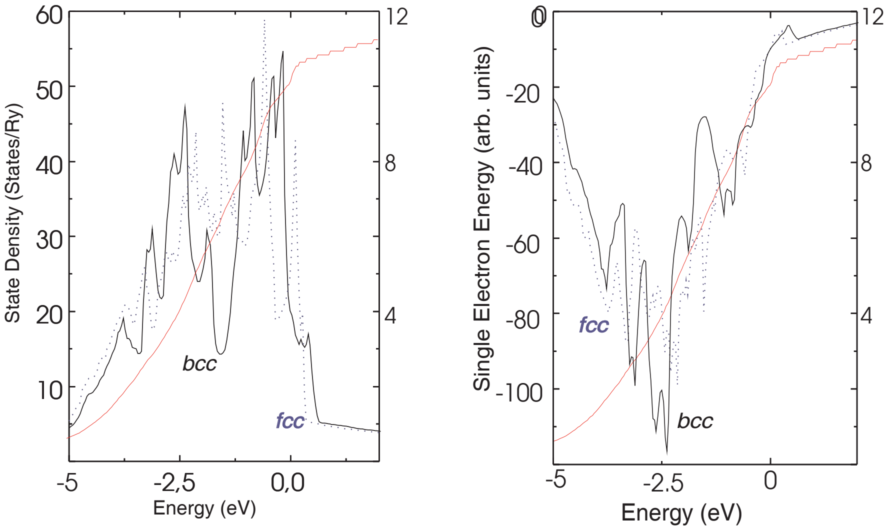

Figure 6. State densities for fcc and bcc transition metals, calculated from a self-consistent potential for Ni, and the difference in the sum energy eigenvalues as a function of band filling.

structure relative to that of the bcc and hcp structures is negative in the middle of the transition metal series (Pettifor, 1995). The much smaller energy difference between the fcc and hcp structures is due to the difference in their sixth moments. After the beginning of the series and for between 6 and 8 states the energy of the hcp structure lies lower whereas the energy of the fcc structure is lower than hcp (but higher than bcc) in the middle of the series and is again the lowest for between about 8 and 9 states and right at the beginning of the series (Pettifor, 1995).

The elements V, Nb, Ta, Cr, Mo and W (n = 5 - 6) therefore have the bcc structure. The elements Ti, Zr, Hf , Mn, Tc, Re, Fe, Ru ,Os ($n = 4$ and 8) should have the hcp structure and the bcc structure of Fe and the α-Mn structures are anomalous. The elements Co, Rh and Ir ($n = 9$) should have the fcc structure and the hcp structure of Co is also anomalous. The crystal structures of several magnetic transition metals are therefore anomalous compared with their isovalent counterparts. Fe, Co and Ni are magnetic because, with $3d$-bandwidths of about 5 eV and Stoner exchange integrals of about 1 eV they obey the Stoner criterion for ferromagnetism (albeit in the case of Fe this is due to an anomalously large peak at the Fermi energy for the bcc structure). The elements Cr and Mn obey the criterion for anti-ferromagnetism which is less stringent towards the centre of a series. Fe, Co and Ni are known from self-consistent calculations to have about 7.4, 8.4 and 9.4 $3d$-electrons, respectively. They are essentially saturated ferromagnets with moments of 2.2, 1.4 and 0.6, respectively, corresponding to a filled spin up band with the moments equal to the number of holes in the spin down band. The fact that the spin up band is filled removes its contribution to bonding and the bonding contribution to both the cohesive energy and crystal structure. The cohesive energies of these three metals are therefore anomalously small and the crystal structures are altered since the ratio of the number of spin down electrons to the total number of spin down states differs from the ratio of the total number of electrons to the total number of states. In Fe and Co the effective fractional d-band occupancy becomes 2.4/5 and 3.4/5 which puts them in the bcc and hcp regions, respectively. Under pressure Fe undergoes a transition to a non-magnetic hcp phase as the increasing bandwidth reduces the magnetic moment and with it the magnetic energy which stabilizes the bcc phase. Although more complicated, the α-Mn phase is also stabilized by magnetism (Pettifor, 1995). Accurate, self-consistent, calculations yield a paramagnetic fcc ground state with a lower energy than a bcc magnetic ground state for Fe although the energy difference is very small (Wang et al., 1985). Detailed studies of the elastic shear constant, which is related to the structural energy difference between bcc and fcc phases, for Fe have also shown that the absence of a spin up contribution is responsible for the anomalously low bulk modulus and shear elastic constant of Fe (Söderlind et al., 1994).

4 Conduction electrons in rare earth metals

Four approaches have been made to the calculation of conduction electron band structure in the rare earths. In the first, the $4f$ states have been treated as part of the band structure (Harmon, 1979; Norman and Koelling, 1993; Temmerman and Sterne, 1990). This treatment is most suitable for Gd where the seven filled spin-up $4f$-states lie self-consistently below, and the empty spin down f-states above, the Fermi energy. The splitting between these two sets of $4f$-states is easily estimated to be 7 times the $4f$–$4f$ exchange integral ($J_{4f4f} \approx 0.69$ eV) or 4.8 eV. The spin down $4f$-bands are quite close to the Fermi level, raise the state density at the Fermi energy through hybridization with the $5d$ states, and they increase the calculated state density at the Fermi energy to 27 states/Ry compared with a value deduced from measurements (Wells et al., 1974) and assuming no enhancement, of 21.35 states/Ry. The $4f$ character at the Fermi energy in Gd is 5 states/Ry (Singh, 1991) which corresponds to the difference between theory and measurement. The situation is far worse for the other metals since the $4f$-bands always cut the Fermi level.

The second approach has been to treat the $4f$ states as part of the core. Since the $4f$ shell is open the occupation number must be input to the calculations and the electronic structure is calculated self-consistently subject to this constraint. This approach has been used very successfully for the computation of cohesive properties (Skriver, 1985; Wills and Eriksson, 1992; Söderlind et al., 1995). The calculated partial $5d$ occupation numbers were found to increase across the series with increasing atomic number leading to the structural sequence hcp → dhcp → Sm-structure → fcc as is to be expected for a $5d$ transition metal series. The $4f$ spin occupation numbers are determined by applying the standard Russell–Saunders coupling scheme to the $4f$ shell and the magnetic moment is given by $\mu_{4f} = g_J J$. The ground state spin component of the total $4f$ moment, μ^s_{4f}, is obtained from the projection of the spin along the direction of total angular momentum

$$\mu^s_{4f} = 2(g_J - 1)J. \tag{11}$$

The $4f$ spin up and spin down occupation numbers are then determined by

$$\begin{aligned} n_{4f} &= n^+_{4f} + n^-_{4f} \\ \mu^s_{4f} &= n^+_{4f} - n^-_{4f} \end{aligned} \tag{12}$$

where $n^{\pm}_{4f}$ are the up and down spin occupation numbers and n_f is the total number of $4f$ electrons. The occupation numbers n^+_{4f}, n^-_{4f} are part of the input to the calculations and are not determined ab initio as are the partial occupation numbers of the conduction electron states.

The third approach, which is more recent, is to incorporate the self-interaction correction (Heaton et al., 1983) (SIC) in the energy band calculations. The result is that localized states are localized further, and the energies of occupied and unoccupied states are split. Svane and Gunnarsson (1990) have applied SIC to the transition metal oxides, obtaining a drastic improvement in band gaps and calculated moments compared with the results of LSDA. The most favourable aspect of SIC in its application to rare earths is the existence of separate occupied and unoccupied states. Szotek et al. (1993) have applied SIC to praseodymium metal where the occupied $4f$ states are pulled well below the conduction bands and the unoccupied $4f$ bands lie about 1 eV above the Fermi energy.

The fourth approach (Thalmeier and Falikov, 1979; Anisimov et al., 1993; Liechtenstein et al., 1994) has become known as 'LDA+U' since it is an attempt to add some aspects of the Hubbard model to self-consistent energy band calculations. An additional interaction of the Hubbard form, which is dependent upon the occupation of the individual orbitals is added. The effect is to make the energies of the individual orbitals dependent upon their occupation, introducing an additional symmetry breaking. This approximation can therefore lead to a large energy separation between occupied and unoccupied states. The electron–electron interaction parameter U which enters the theory may be estimated from constrained density functional calculations.

Most of the LSDA calculations have been for Gd metal. For calculations with the $4f$-states polarized in the bands (Harmon, 1979; Norman and Koelling, 1993; Temmerman and Sterne, 1990; Sticht and Kübler, 1985; Krutzen and Springelkamp, 1989; Richter and Eschrig, 1989) there is agreement that the state density at the Fermi energy is 25–37 states/Ry/atom/spin, to which there is a $4f$ contribution of about 5–6 states/Ry/atom/spin. From calculations with a paramagnetic ground state and the $4f$ states in the core (Harmon, 1979; Norman and Koelling, 1993; Temmerman and Sterne, 1990; Lindgård, 1976; Brooks et al., 1992) the state density at the Fermi energy per atom was found to be between 22 and 28 states/Ry/atom/spin. From calculations with the $4f$ states polarized in the core (Brooks et al., 1992) or an exchange splitting applied (Skriver and Mertig, 1990) the state density at the Fermi energy was calculated to be 12 states/Ry/atom/spin. The latter calculations yield results that are on the correct side of experiment. The calculated magnetic moments are in good agreement with measurements (Roeland et al., 1975) of 7.63 μ_B lying between 7.65 μ_B and 7.68 μ_B (Sticht and Kübler, 1985; Krutzen and Springelkamp, 1989; Temmerman and Sterne, 1990; Richter and Eschrig, 1989; Brooks et al., 1992).

Fermi surface calculations for Gd (Harmon, 1979; Norman and Koelling, 1993; Temmerman and Sterne, 1990; Singh, 1991; Ahuja et al., 1994) are in reasonable agreement with measurements (Young et al., 1973; Schirber et al., 1976; Young et al., 1976; Mattocks and Young, 1977; Sondhelm and Young, 1985) except that some measured smaller orbits provide some difficulty. Detailed dHvA experiments (Wulff et al., 1988) on dhcp praseodymium have led to calculations (Wulff et al., 1988; Auluck and Brooks, 1991) of its Fermi surface for which there is reasonable agreement with the frequencies of the measured orbits.

5 Rare earth transition metal intermetallics

5.1 The ReFe$_2$ series

Most studies have been for lutetium or yttrium compounds (Coehoorn, 1991; Cyrot and Lavagna, 1979; Yamada, 1988; Szpunar and Jr, 1990; Jaswal, 1990; Sellmyer et al., 1988) which simulate the conduction electron band structure of many rare earth compounds well. Fig. 7 shows the calculated total conduction electron spin moment through the RFe$_2$ series and its decomposition into $3d$ and $5d$ contributions (Brooks et al., 1991a). The individual $5d$ and $3d$ moments depend much more

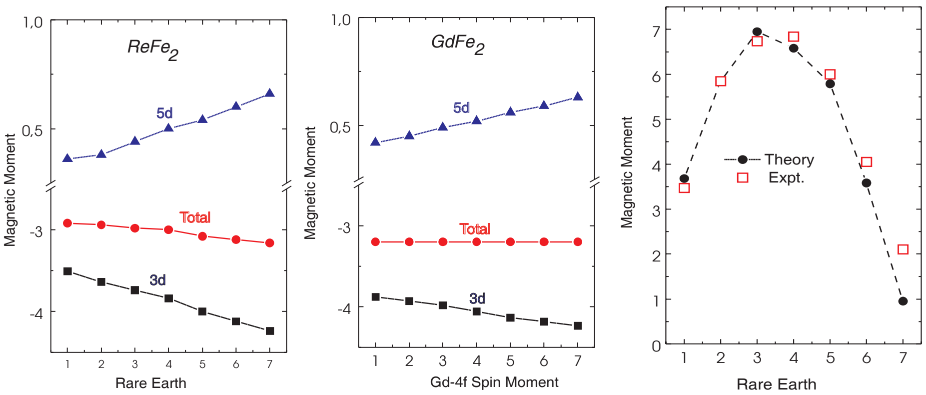

Figure 7. Calculated and measured moments of the ReFe$_2$ series plus the conduction electron contributions analysed into $3d$ and $5d$ contributions.

strongly upon atomic number than does the total moment. Also shown are the results of calculations for GdFe$_2$ when the magnitude of the $4f$ spin moment is constrained to vary from seven to zero. The calculated number of $5d$ electrons is found to be independent of the size of the $4f$ spin. Both the $5d$ and $3d$ moments increase when the $4f$ spin moment is increased but, as they are of opposite sign, the changes cancel and the total conduction electron moment remains constant, suggesting that the total conduction electron moment is saturated. The good agreement between the calculated total (including $4f$) moments and measurements is also shown in Fig. 7.

A simple model illustrates the origin of the ferrimagnetic interaction. In the free atom the energy of the $3d$ states lies far lower than that of the $5d$ states. When the solid is formed the $5d$ and $3d$ states hybridize, yielding the bonding-antibonding level scheme illustrated in Fig. 8. The bonding level is primarily of $3d$ character while the antibonding level has mainly $5d$ character. The degree of mixing between the $3d$ and $5d$ states depends on the overlap matrix element and on the energy separation between the $3d$ and $5d$ levels. When the $3d$ electrons polarize the energy difference between the bonding and antibonding sub-bands differs for the two spin directions, changing the $3d$–$5d$ hybridization for the majority and minority spins. The $5d$ content in the spin-up $3d$ bonding band decreases and that of spin-down $3d$ bonding band increases. Therefore the $3d$ and $5d$ spins must be in anti-parallel.

When there is a localized $4f$ spin it must be parallel to the $5d$ spin and $4f$–$5d$ exchange enhances the total $5d$ moment by moving the $5d$ spin up band further

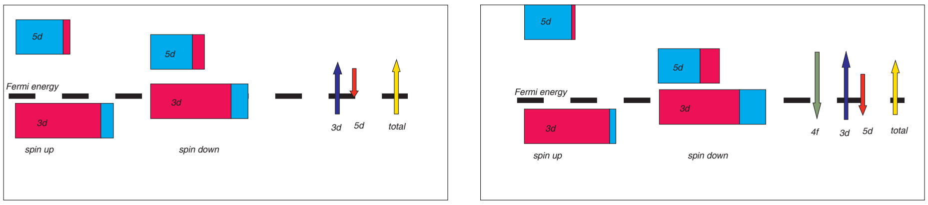

Figure 8. Model partial $3d$ and $5d$ state densities for RT_2 compounds showing the effect of the introduction of a $4f$ moment which polarizes the $5d$ states. The electron contributions analysed into $3d$ and $5d$ contributions.

away from the spin-up $3d$ bonding band, reducing $3d$–$5d$ spin-up hybridization. The opposite occurs for the spin-down bands the net result of which is that spin is transferred to the $3d$ sites and the $3d$ moment increases. However, if the total conduction electron moment is saturated, only its distribution between the R and Fe atoms changes. Therefore the presence of the $4f$ spin redistributes the conduction electron spin between the rare-earth and iron sites, while the total moment remains constant. This cancellation explains the successful interpretation of experimental magnetic moment data in terms of a constant conduction electron spin and an atomic $4f$ moment through a series of compounds.

5.2 Rare earth–transition metal exchange interactions

The $3d$–$5d$ hybridization not only produces significant $5d$ density at the R-sites but is also responsible for the crucial coupling between the R and M moments. The essential point to realize is that the R–$4f$ and R–$5d$ spins are coupled by local exchange interactions (which are always ferromagnetic) and that the interaction between R–$4f$ and M–$3d$ spins is mediated entirely by the R–$5d$ M–$3d$ hybridization (Brooks et al., 1991c).

The energy of the conduction electrons is at a variational minimum for a self-consistent calculation in which the $4f$ moment is constrained. The total energy change due to changes in conduction electron moment is therefore $o(\delta\mu_c^2)$ since individual contributions from exchange, kinetic and potential energies must cancel to $o(\delta\mu_c)$. This cancellation due to the variational principle allows the molecular field from the transition metal at the rare earth site to be calculated particularly simply. A change of $4f$ spin induces changes in conduction electron moment as the conduction electrons move to shield the disturbance, but the resulting total energy change is dominated by the explicit change of $4f$–$5d$ spin polarization energy due to the change of $4f$ spin which is the only contribution of $o(\delta\mu_c)$. The spin polarization energy between $4f$ and $5d$ states is

$$E_{4f5d} = -\frac{1}{2} J_{4f5d} \mu^s_{4f} \mu_{5d} \,. \tag{13}$$

Neutron scattering experiments on the RFe$_2$ series have resolved the low lying spin wave modes and the generic form of the spectra is shown in Fig. 9. The lowest mode (labelled 1) at zero wave vector is the uniform mode and the highest (labelled 3) the exchange resonance mode of a ferrimagnet. The mode of interest here is the dispersionless mode (labelled 2) which corresponds to the precession of the R–$4f$ moments in the molecular field due to the M-moments. The molecular field is therefore about 10 meV. Contact between Eq. (13) and experiment is established through this spin wave gap. Equation (13) may be re-written in terms of the total $4f$ angular momentum via the Wigner–Eckart theorem

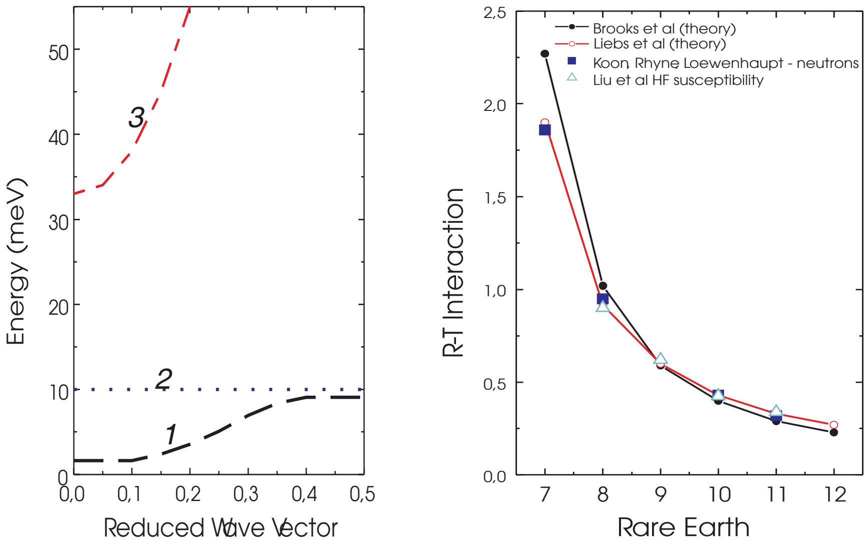

Figure 9. Schematic spin wave spectrum for a RFe$_2$ compound and the calculated and measured inter-atomic exchange interaction.

$$E_{4f5d} = -2(g_J - 1) J_{4f5d} \bar{J}_{4f} \bar{S}_{5d} \tag{14}$$

and, since the selection rule for spin waves is $\Delta J = \pm 1$, the change in total energy is the gap. Due to the above mentioned cancellation theorem the change of total energy to $o(\delta m)$ is

$$\Delta = 2(g_J - 1)J_{4f5d}\bar{S}_{5d}\,. \tag{15}$$

The results are compared with experiment in Fig. 9. The experimental results were from neutron scattering (Koon and Rhyne, 1980; Nicklow et al., 1976), high field susceptibility (Liu et al., 1991) or Curie temperature (Belorizky et al., 1988) measurements. The values of the decrease in exchange interaction is due to both a decrease in the bare exchange integrals – caused by lanthanide contraction – and the decrease in $5d$ spin across the series, which itself is caused by the decrease in $4f$ moment. Although the parameters in Eq. (13) appear to be properties of the R atoms, in fact the R–$5d$ density arises from hybridization with the M–$3d$ states and this is the origin of the interatomic interactions.

5.3 Other rare earth compounds

Several electronic structure calculations for $Nd_2Fe_{14}B$ have been made (Coehoorn, 1991; Cyrot and Lavagna, 1979; Yamada, 1988; Szpunar and Jr, 1990; Jaswal, 1990; Sellmyer et al., 1988; Nordström et al., 1991; Hummler and Fähnle, 1992) and both the $4f$ states of Nd and the $3d$ states of Fe have been spin polarized. The total moment of the unperturbed $4f^3$ shell of Nd is 3.27 μ_B/atom. This consists of a projected orbital part of 5.72 μ_B/atom and a projected spin contribution of -2.45 μ_B/atom. The size of the conduction electron rare-earth moment increases by about 50 per cent due to the $4f$ spin moment.

The conduction bands in RCo_2 compounds (Coehoorn, 1991; Cyrot and Lavagna, 1979; Yamada, 1988; Szpunar and Jr, 1990; Jaswal, 1990; Sellmyer et al., 1988; Wohlfarth and Rhodes, 1962; Shimizu, 1964; Schwarz and Mohn, 1984) are metamagnetic. The state density of the RCo_2 compounds is almost identical to the state density of YCo_2. The Fermi energy lies in a dip in the state density with a large double peak just below and a somewhat broader peak above. The criterion for the local stability of a metamagnetic state is given in terms of the high field unenhanced susceptibility by

$$\frac{1}{2I}\left[\frac{1}{N^+(E_F)} + \frac{1}{N^-(E_F)}\right] \le 1.$$

At a finite splitting of the energy bands both spin up and spin down state densities become large enough to satisfy this criterion. A similar situation occurs for $Y(Fe_{1-x}Co_x)_2$ alloys.

The exchange enhanced paramagnetism of the Co $3d$-bands in RCo_2 compounds was studied (Coehoorn, 1991; Cyrot and Lavagna, 1979; Yamada, 1988; Szpunar and Jr, 1990; Jaswal, 1990; Sellmyer et al., 1988; Bloch et al., 1975) in an attempt to explain the trend in Curie temperatures across the heavy rare earth series, the first order magnetic transitions observed for $ErCo_2$, $HoCo_2$ and $DyCo_2$, and the second order magnetic transitions observed for $TbCo_2$ and $GdCo_2$, in terms of a molecular field theory in which the $3d$ band susceptibility is enhanced by the field from the localized $4f$-moment. The d-band susceptibility was calculated (Nordström et al., 1992a) to be about 10 States/Ry/atom in $GdFe_2$ and fairly constant across the series. The calculated Curie temperature of $GdCo_2$ is then 413 K compared with a measured value of 395 K.

5.4 Cerium compounds

Several cerium compounds have anomalously small lattice constants, Curie temperatures that are low in comparison with the other isostructural rare-earth compounds and magnetic moments that deviate from the values one would expect for normal trivalent ions at the cerium sites. Self-consistent LMTO calculations (Eriksson et al., 1988) for the CeM_2 (M = Fe, Co and Ni) cubic Laves phases with the $4f$ states treated as itinerant reproduce the trends in lattice constant. Only $CeFe_2$ is calculated to satisfy the Stoner criterion, in agreement with experiment, with a calculated total spin moment of 2.16 μ_B/f.u. which is about 1 μ_B less than the calculated total conduction electron moment for $GdFe_2$ of 3.15 μ_B/f.u. When the $4f$ electrons are itinerant a $4f$ electron is transferred from the core to the valence band states. If the conduction band moment is saturated the extra valence electron must enter the spin down states, reducing the total moment by 1 μ_B/f.u. The reduction of the moment is probably the reason for the anomalously low Curie temperatures of many of the cerium intermetallic ferromagnets. A similar moment reduction was found for (Nordström et al., 1990) $CeCo_5$. This reduction for $CeCo_5$ is caused by the hybridization between the Ce–$4f$ and the Co–$3d$ states which induces a $4f$ spin moment antiparallel to the cobalt moment and reduces the cobalt moment which is less than for $LaCo_5$, as is observed experimentally The Curie temperature for $CeCo_5$ is about 200 K less than would be expected from comparison with the other RCo_5 compounds.

6 Orbital magnetism of conduction electrons

The orbital contribution to the magnetic moment is 0.08 μ_B, 0.14 μ_B and 0.05 μ_B in Fe, Co and Ni, respectively (Stearns, 1986; Bonnenberg et al., 1986). The orbital moments are parallel to the spin contributions of 2.13 μ_B, 1.52 μ_B and 0.57 μ_B for Fe, Co and Ni, respectively (Fig. 10). The orbital moment belongs almost entirely to the $3d$ electrons. The spin contributions to the magnetic moments are

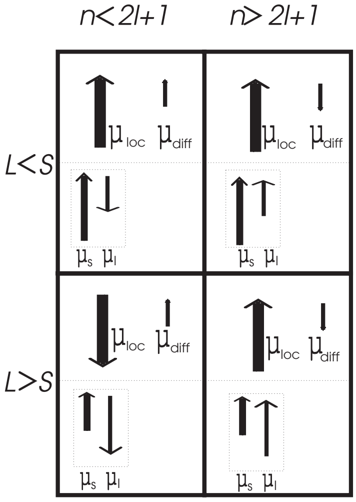

Figure 10. The relative signs of the local, spin and orbital, and diffuse moments of early and late transition metals.

resolved into local, or 3*d*, and diffuse, or *sp*, parts in Fig. 10. The *diffuse* part of the moment lies mainly in the interstitial region of the crystal and is not detected in neutron diffraction experiments. In Fe, Co and Ni the diffuse part of the moment is antiparallel to the local part. The origin of the relative signs of the diffuse and local moments is hybridization between the 3*d* and *sp* electrons. The Fe, Co and Ni 3*d* band is more than half-filled and the Fermi energy lies close to the bottom of the broad, free electron like, *sp* bands. The hybridization is therefore similar to that between early and a late transition metals and results in the relative sign of the local and diffuse moments being antiparallel (Terakura, 1977; Anderson, 1961; Heine and Samson, 1980).

Magnetism in actinide compounds is characterized by two unusual features. The first is the presence of correlations associated with very narrow bands and the second is the effect of relatively large spin–orbit interaction for the 5*f* electrons. In contrast to the theory for the transition metals, spin–orbit interaction plays a first-order role in the theory of magnetism and moment formation in the actinides. The actinides are early transition metals and the 4*f* moments are polarized parallel to the 5*d* moments which constitute nearly all of the diffuse moment. Exchange interactions between the local and diffuse moments are always positive and would always lead to parallel polarization in the absence of hybridization. In Fe, Co and Ni the spin moments are not large and the exchange interactions between local and diffuse moments small enough that hybridization dominates. In the actinides both mechanisms lead to parallel polarization of the local and diffuse moments, Fig. 10.

In Fe, Co and Ni the orbital contributions to the moments are parallel to the spin contributions since the $3d$ bands are more than half filled, Fig. 10. Light actinides have a less than half-filled $5f$ band, therefore the induced orbital moment is antiparallel to the $5f$ spin moment, Fig. 10. Therefore there are two sign changes – for both diffuse and orbital moments – occurring between the right and left hand sides of Fig. 10.

Relativistic energy band calculations yield orbital contributions which are larger than the spin contributions to the moments in compounds containing actinides (Brooks and Kelly, 1983; Brooks, 1985; Eriksson et al., 1990a,c; Severin et al., 1991; Norman and Koelling, 1986; Norman et al., 1988). The induced orbital moment is sensitive to the ratio of bandwidth to spin–orbit interaction which is far smaller in the actinides than transition metals. The spin–orbit splitting of the $5f$ states in uranium is about 0.77 eV, which is comparable with the Stoner splitting. However, although the calculated orbital moments are very large in actinides, they are smaller than measured. This is also true in Fe, Co and Ni, although the larger discrepancies for the actinides are more obvious.

In the homogeneous electron gas for which the interactions in LSDA are derived, there is no spin–orbit interaction as there is no localized nuclear charge. The orbital exchange interactions, Coulomb in nature, which occur in atoms do not occur in the free electron gas. Orbital exchange interactions lead to interactions between the atomic orbital moments which are responsible for Hund's second rule. Hund's first rule, the exchange interaction between spins, is reproduced in LSDA where it leads to spin polarization. The interaction between the orbital moments is absent in LSDA. One way to approximate orbital interactions which has had some success has been suggested (Brooks, 1985; Eriksson et al., 1990a). A Hund's second rule energy which peaks for quarter filled shells and is zero for half-filled shells is added to the Hamiltonian. Its functional dependence upon occupation number may be approximated quite well, but not perfectly, by $-(1/2)E^3L_z^2$ where E^3 is a Racah parameter (a linear combination of Slater Coulomb integrals). Although the orbital polarization energy in this approximation is not a functional of the density it is a function, through L^z – the total orbital angular momentum of the shell, of the orbital occupation numbers. The differential of the orbital polarization energy with respect to occupation number leads to different energies for the orbital levels $|m\rangle$ when there is an orbital moment. E^3, the Racah parameter, may be re-evaluated during the iterative cycles of a self-consistent calculation along with the orbital occupation numbers, so that no free parameters are introduced. Therefore orbital interactions arise by consideration of a series of Hund's rule ground states with single determinant wave functions. The orbital interactions are exchange interactions just as are the spin interactions and they arise from preferential filling of orbitals. This approximation has been applied to a number of systems where it improves agreement between theory and experiment. Applications to non-actinides such as Fe, Co and Ni and some cobalt compounds have also improved agreement with experiment for the orbital moments.

The magnetic anisotropy energy is usually calculated by making two sets of calculations with the quantization axis along hard and easy axes and subtracting the total energies for the two directions. For Fe, Co and Ni the calculation of magnetic anisotropy has been only partially successful (Daalderop et al., 1990; Jansen, 1990). Part of the difficulty is because the magnetic anisotropy energy for these systems is of the order of μeV, which demands extremely accurate numerical treatment. The magnitude of the MAE is calculated to be too small and in Ni the sign is wrong. Inclusion of the orbital polarization correction term improves the results, except for Ni. For rare earth compounds (Daalderop et al., 1992; Nordström et al., 1992b) and, for actinide compounds (Brooks et al., 1986) the situation is better. For example, the anisotropy of US was about double that measured. The anisotropy energy of US is about two orders of magnitude greater than that of a rare earth metal.

Acknowledgements

Much of the personal contribution described in this article was made in collaboration with Börje Johansson, Hans Skriver, Olle Eriksson and Lars Nordström, frequently under the critical but sympathetic eye of Allan Mackintosh whose interest and encouragement will be sorely missed but not forgotten.

References

Ahuja R, Auluck S, Johansson B and Brooks MSS, 1994: Phys. Rev. B **50**, 5147

Andersen OK, 1975: Phys. Rev. B **12**, 3060

Anderson PW, 1961: Phys. Rev. **124**, 41

Anisimov VI, Soloyev IV, Korotin MA, Czyzyk MT and Sawatzky GA, 1993: Phys. Rev. B **48**, 16929

Auluck S and Brooks MSS, 1991: (unpublished)

Belorizky E, Gavigan JP, Givord D and Li HS, 1988: Europhys. Lett. **5**, 349

Bloch D, Edwards DM, Shimizu M and Voiron J, 1975: J. Phys. F **5**, 1217

Bonnenberg D, Hempel KA and Wijn HPJ, 1986: in *3d, 4d and 5d Elements, Alloys and Compounds*, ed. H. Wijn (Springer Verlag, Berlin) Landolt–Börnstein, New Series, group 3, Vol. 19a

Boucherle JX, Givord D and Schweizer J, 1982: J. Phys. (Paris) C **7**, 199

Brooks MSS, 1985: Physica B **130**, 6

Brooks MSS and Johansson B, 1993: in *Handbook of Magnetic Materials*, ed. K. Buschow (Elsevier Science Publishers) Vol. 7, p. 139

Brooks MSS and Kelly PJ, 1983: Phys. Rev. Lett. **51**, 1708
Brooks MSS, Johansson B, Eriksson O and Skriver HL, 1986: Physica B **144**, 1
Brooks MSS, Eriksson O and Johansson B, 1989: J. Phys. Condens. Matter **1**, 5861
Brooks MSS, Gasche T, Auluck S, Nordström L, Severing L, Trygg L and Johansson B, 1991a: J. Appl. Phys. **79**, 5972
Brooks MSS, Nordström L and Johansson B, 1991b: J. Phys. Condens. Matter **3**, 2357
Brooks MSS, Nordström L and Johansson B, 1991c: J. Phys. Condens. Matter **3**, 3393
Brooks MSS, Auluck S, Gasche T, Trygg L, Nordström L, Severing L and Johansson B, 1992: J. Magn. Magn. Mater. **104-107**, 1496
Christensen NE, Gunnarsson O, Jepsen O and Andersen OK, 1988: J. Phys. (Paris) C **8**, 17
Coehoorn R 1991: in *Supermagnets, Hard Magnetic Materials*, eds. G. Long and F. Grandjean, (Kluwer Academic, Dordrecht)
Cyrot M and Lavagna M, 1979: J. Phys. (Paris) **40**, 763
Cyrot-Lackmann F, 1967: Adv. Phys. **16**, 393
Daalderop GHO, Kelly PJ and Schuurmans MFH, 1990: Phys. Rev. B **42**, 11919
Daalderop GHO, Kelly PJ and Schuurmans MFH, 1992: J. Magn. Magn. Mater. **104-107**, 737
Ducastelle F and Cyrot-Lackmann F, 1971: J. Phys. Chem. Solids **32**, 285
Duthie JC and Pettifor DG, 1977: Phys. Rev. Lett. **38**, 564
Ebert H, Strange P and Gyoffry BL, 1988: J. Phys. F **18**, L135
Eriksson O, Nordström L, Brooks MSS and Johanson B, 1988: Phys. Rev. Lett. **60**, 2523
Eriksson O, Brooks MSS and Johansson B, 1990a: Phys. Rev. B **41**, 9087
Eriksson O, Johansson B, Albers RC, Boring AM and Brooks MSS, 1990b: Phys. Rev. B **42**, 2707
Eriksson O, Johansson B and Brooks MSS, 1990c: Phys. Rev. B **41**, 9095
Friedel J, 1969: in *The Physics of Metals*, ed. J. Ziman, (Cambridge Univ. Press) p. 341
Givord D, Gregory AR and Schweizer J, 1980: J. Magn. Magn. Mater. **15-18**, 293
Givord D, Li HS and Tasset F, 1985: J. Appl. Phys. **57**, 4100
Gunnarsson O, 1976: J. Phys. F **6**, 587
Gunnarsson O, 1977: Physica B **91**, 329
Harmon BN, 1979: J. Phys. (Paris) C **5**, 65
Heaton RA, Harrison JG and Lin CC, 1983: Phys. Rev. B **28**, 5992
Heine V and Samson JH, 1980: J. Phys. F **10**, 2609
Hill HH, 1970: in *Plutonium 1970*, ed. W. Miner (Met. Soc. AIME, New York) p. 2
Hohenberg P and Kohn W, 1964: Phys. Rev. **136**, 864
Hummler K and Fähnle M, 1992: Phys. Rev. B **45**, 3161
Jansen HJF, 1990: J. Appl. Phys. **67**, 4555
Jaswal SS, 1990: Phys. Rev. B **41**, 9697
Jensen J and Mackintosh AR, 1991: *Rare Earth Magnetism: Structures and Excitations* (Clarendon Press, Oxford)
Kohn W and Sham LJ, 1965: Phys. Rev. A **140**, 1133
Koon NC and Rhyne JJ, 1980: in *Crystalline Electric Field and Structural Effects*, eds. J. Crow, P. Guertin and T. Mihalisin, (Plenum, New York) p. 125
Krutzen BCH and Springelkamp F, 1989: J. Phys. Chem. **1**, 8369
Liebs M, Hummler K and Fähnle M, 1993: J. Magn. Magn. Mater. **124**, 239
Liechtenstein AI, Antropov VP and Harmon BN, 1994: Phys. RevḂ **49**, 10770
Lindgård PA, 1976: in *Metals and Metallic Compounds*, eds. J. Lopuzanski, A. Pekalsky and J. Przystawa (Plenum, New York) p. 203
Liu JP, de Boer FR and Buschow KHJ, 1991: J. Magn. Magn. Mater. **98**, 291
Mackintosh AR and Andersen OK, 1979: (Cambridge Univ. Press) p. 149
Mattocks PG and Young RC, 1977: J. Phys. F **7**, 1219

Nicklow RM, Koon NC, Williams CM and Milstein JB, 1976: Phys. Rev. Lett. **36**, 532

Nordström L, Eriksson O, Brooks MSS and Johansson B, 1990: Phys. Rev. B **41**, 911

Nordström L, Johansson B and Brooks MSS, 1991: J. Appl. Phys. **69**, 5708

Nordström L, Brooks MSS and Johansson B, 1992a: J. Magn. Magn. Mater. **104-107**, 1378

Nordström L, Brooks MSS and Johansson B, 1992b: J. Magn. Magn. Mater. **104-107**, 1942

Norman MR and Koelling DD, 1986: Phys. Rev. B **33**, 3803

Norman MR and Koelling DD, 1993: in *Handbook of Physics and Chemestry of Rare Earths*, eds. K.A. Gsneidner, L. Eyring, G. Lander and G. Choppin (North Holland, Amsterdam) Vol. 17, p. 1

Norman MR, Min BI, Oguchi T and Freeman AJ, 1988: Phys. Rev. B **38**, 6818

Pettifor DG, 1970: J. Phys. C **C3**, 367

Pettifor DG, 1972: in *Metallurgical Chemestry*, ed. O Kubashewsky, (H.M. Stationary Office, London)

Pettifor DG, 1976: Commun. Phys. **1**, 141

Pettifor DG, 1986: J. Phys. Chem. **19**, 285

Pettifor DG, 1995: *Bonding and Structure of Molecules and Solids* (Clarendon Press, Oxford) p. 223

Richter M and Eschrig H, 1989: Solid State Commun. **72**, 263

Roeland LW, Cock GJ, Muller FA, Moleman CA, McEwen KA, Jordan RC and Jones DW, 1975: J. Phys. F **5**, L233

Schirber JE, Schmidt FA, Harmon BN and Koelling DD, 1976: Phys. Rev. Lett. **36**, 448

Schwarz K and Mohn P, 1984: J. Phys. F **14**, L129

Sellmyer DJ, Engelhardt MA, Jaswal SS and Arko AJ, 1988: Phys. Rev. Lett. **60**, 2077

Severin L, Nordström L, Brooks MSS and Johansson B, 1991: Phys. Rev. B **44**, 9392

Severin L, Brooks MSS and Johansson B, 1993: Phys. Rev. Lett. **71**, 3214

Shimizu M, 1964: Proc. Phys. Soc. **86**, 147

Singh DJ, 1991: Phys. Rev. B **44**, 7451

Singh M, Callaway J and Wang CS, 1976: Phys. Rev. B **14**, 1214

Skriver HL, 1983a: in *Systematics and Properties of the Lanthanides*, ed. S. Sinha (Reidel, Dordrecht) p. 213

Skriver HL, 1983b: *Muffin Tin Orbitals and Electronic Structure* (Springer Verlag, Heidelberg)

Skriver HL, 1985: Phys. Rev. B **31**, 1909

Skriver HL and Mertig I, 1990: Phys. Rev. B **41**, 6553

Skriver HL, Andersen OK and Johansson B, 1978: Phys. Rev. Lett. **41**, 42

Skriver HL, Andersen OK and Johansson B, 1980: Phys. Rev. Lett. **44**, 1230

Söderlind P, Ahuja R, Eriksson O, Willis JM and Johansson B, 1994: Phys. Rev. B **50**, 5918

Söderlind P, Wills JM, Johansson B and Eriksson O, 1995: Nature **374**, 524

Sondhelm SA and Young RC, 1985: J. Phys. F **15**, L261

Stearns MB, 1986: in *3d, 4d and 5d Elements, Alloys and Compounds*, ed. H. Wijn (Springer Verlag, Berlin) Landolt–Börnstein, New Series, group 3, Vol. 19a

Sticht J and Kübler J, 1985: Solid State Commun. **53**, 529

Svane A and Gunnarsson O, 1990: Phys. Rev. Lett. **65**, 1148

Szotek Z, Temmerman WM and Winter H, 1993: Phys. Rev. B **47**, 1124

Szpunar B and Jr VHS, 1990: J. Solid State Chem. **88**, 217

Temmerman WM and Sterne PA, 1990: J. Phys. Chem. **2**, 5529

Terakura K, 1977: J. Phys. F **7**, 1773

Thalmeier P and Falikov LM, 1979: Phys. Rev. B **20**, 4637

von Barth U and Hedin L, 1972: J. Phys. Chem. **5**, 1629

Wang CS, Klein B and Krakauer H, 1985: Phys. Rev. Lett. **54**, 1852

Wells P, Lanchester PC, Jones WD and Jordan RG, 1974: J. Phys. F **4**, 1729

Wills J and Eriksson OK, 1992: Phys. Rev. B **45**, 13879
Wohlfarth P and Rhodes P, 1962: Phil. Mag. **7**, 1817
Wulff M, Lonzarich GG, Fort D and Skriver HL, 1988: Europhys. Lett. **7**, 629
Yamada H, 1988: Physica B **149**, 390
Yamada H and Shimizu M, 1986: J. Phys. F **16**, 1039
Young RC, Jordan RG and Jones DW, 1973: Phys. Rev. Lett. **31**, 1473
Young RC, Jordan RG and Jones DW, 1976: J. Phys. F **6**, L37